

SYNTHESIS, CHARACTERIZATION, LIPOXYGENASE, AND TYROSINASE INHIBITORY ACTIVITIES OF NON-CYTOTOXIC TITANIUM(III) AND (IV) HYDRAZIDE COMPLEXES

Zara Shaikh¹, Uzma Ashiq¹, Rifat Ara Jamal², Sana Gul³, Mohammad Mahroof-Tahir³, Sadaf Sultan¹, Uzma Salar⁴ and Khalid Mohammed Khan^{5,6*}

¹Department of Chemistry, University of Karachi, Karachi 75270, Pakistan

²Department of Chemistry, Federal Urdu University of Art, Science and Technology, Karachi, Pakistan

³Department of Chemistry and Earth Sciences, Qatar University, Doha, Qatar

⁴Dr. Panjwani Center for Molecular Medicine and Drug Research, International Center for Chemical and Biological Sciences, University of Karachi, Karachi-75270, Pakistan

⁵H. E. J. Research Institute of Chemistry, International Center for Chemical and Biological Sciences, University of Karachi, Karachi-75270, Pakistan

⁶Department of Clinical Pharmacy, Institute for Research and Medical Consultations (IRMC), Imam Abdulrahman Bin Faisal University, P.O. Box 1982, Dammam, 31441, Saudi Arabia

(Received December 7, 2021; Revised November 2, 2022; Accepted November 3, 2022)

ABSTRACT. Ti(III) and (IV) hydrazide complexes were synthesized, characterized, and screened for their tyrosinase and lipoxygenase inhibitory and cytotoxic activities. The geometry of Ti(III) hydrazide complexes is tentatively assigned as octahedral. Magnetic moments were found around 1.7 B.M. and electronic spectral transition in the range of 495-518 nm. Evaluation of Ti(IV) and Ti(III) hydrazide complexes for tyrosinase and lipoxygenase inhibitory activities revealed varying inhibition potential. Hydrazide ligands were inactive against tyrosinase, while significant activity was observed against lipoxygenase (LOX). Good to moderate inhibition activity was observed by Ti(IV) and Ti(III) hydrazide complexes against both enzymes. At the same time, promising results were obtained for Ti(IV) hydrazide complexes against tyrosinase enzymes suggesting their broad application as tyrosinase inhibitors. Complex **4d** possess negative inhibition, thus behaving as a tyrosinase activator. The docking results showed a good correlation between complex experimental activities and binding energies. Cytotoxic investigation revealed the non-toxicity of complexes against normal cells.

KEY WORDS: Titanium(III) and titanium(IV) hydrazide complex, Tyrosinase, Lipoxygenase, Inhibition, Molecular docking, Cytotoxicity

INTRODUCTION

Hydrazides and their transition metal complexes are of astonishing consideration to researchers. They serve as the imperative biological model due to their notable bioactivities, such as antibacterial, herbicidal, antitumor, and antifungal. In hydrazides, C=O (the carbonyl moiety) is suggested to be the responsible component for such activities [1]. Furthermore, like other metal hydrazide complexes, titanium hydrazide complexes have also been reported to possess excellent biological potential like anticancer, antioxidative, photocatalytic, and whitening agent properties [2-4]. Therefore, discovering new biologically active titanium complexes is essential to explore their applications as novel drugs.

Cancer has become a severe problem and the second leading cause of death in public healthcare. Chemotherapy using cytotoxic drugs is the most commonly applied treatment to cure this disease. Cytotoxicity is the degree of a compound exhibits a toxic effect on living healthy cells resulting in several cell fates like necrosis, apoptosis, or reduction in cell viability. In a cytotoxic reaction, a non-cytotropic antibody is tagged with foreign antigen on the cell surface,

*Corresponding author. E-mail: khalid.khan@iccs.edu, drkhalidhej@gmail.com

This work is licensed under the Creative Commons Attribution 4.0 International License

which activates the complement pathway through the formation of an immune complex, eventually producing cell lysis or cell impairments. For this purpose, novel chemotherapeutic agents must be discovered with potent cytotoxic activity against cancer cells and less toxicity to normal cells. The promising anticancer potential has been observed in a series of titanium compounds like budotitan [5], titanocene dichloride [6], titanium(IV) based complexes with phenol at ligands [7] and Ti(IV) salen complexes [8]. In addition, a series of novel binuclear titanium(IV) complexes, $[\text{Ti}(\text{sal})\text{LI}-\text{V}(\text{OBU})(\mu\text{-OBU})_2]$, are also reported to possess anticancer properties [9].

Tyrosinase (polyphenol oxidase), a copper-containing monooxygenase, is the primary enzyme responsible for the production of melanin which is a major contributor to hair, eye, and skin pigments. Melanin plays a significant role in skin photoprotection against UV-induced injuries [10]. It is also responsible for scavenging free radical species produced within cells [11]. At the same time, its continuous production leads to unfavorable darkening, dermatological disorders, and melanoma, a serious form of cancer. Melasma, freckles, and age spots also cause melanin accumulation [12]. To prevent this browning process, tyrosinase inhibitors are of great importance. Many tyrosinase inhibitors have been described for their wide applications in the cosmetic and food industries [13, 14] and the treatment of skin cancers [15]. Some tyrosinase inhibitors are also found to possess potential antibacterial capabilities [16]. However, tyrosinase activity may also be reduced without inhibition, leading to a decreased concentration of melanin, which results in low protection against UV irradiations and causes skin cancer and other skin ailments like oculocutaneous albinism, hypochromia, vitiligo, and other hypopigmentation disorders. Various studies have overcome this deficiency by searching for tyrosinase activators [17, 18].

Lipoxygenase is the source of many reactive oxygen species; for example, lipid hydroperoxide is generated by lipoxygenase and cyclooxygenase through arachidonic acid metabolism. The mammalian 5-LOX enzyme is responsible for the production of leukotrienes (LTs) and its cysteinyl metabolite leukotriene (cysLT), which act as mediators and bronchoconstrictor of allergic asthma attacks [19]. Another mammalian enzyme, 15-LOX, is reported to participate in chronic obstructive pulmonary disease (COPD) and cancer progression [20, 21]. However, the detailed study of the LOX inhibition mechanism reveals several anticancer and antiinflammatory products. The procarcinogenicity of the LOX enzyme can be shifted to anticarcinogenicity by the combination of LOX modulators through an innovative approach to cancer chemoprevention [19]. Recently, the lipoxygenase enzyme inhibition activity of hydrazide ligands and their Pt(IV) metal complexes have been reported [22].

The present study emphasizes the chemistry, including synthesis and characterization, cytotoxicity, and enzyme inhibition activities (including tyrosinase and lipoxygenase) of titanium and its complexes in oxidation states III and IV. The cytotoxic activity was determined against 3T3 normal fibroblast cells. Molecular docking was also conducted on the 5-LOX and tyrosinase enzymes to evaluate the quantitative relationship between target enzymes and titanium-hydrazide complexes.

EXPERIMENTAL

Materials and methods

Titanium tetrachloride, titanium trichloride, and analytical-grade reagents were purchased from Merck and Sigma Aldrich and used without further purification. All reagent-grade chemicals were used, and organic solvents were purified and dried before use. Infrared spectra were recorded on a Shimadzu 460 IR spectrometer in the range of 4000-400 cm^{-1} using KBr disks. UV-Visible spectra were recorded on Shimadzu 1601 UV-Visible spectrophotometer from 200 to 800 nm at room temperature. Carbon, hydrogen, and nitrogen analyses were performed on a PerkinElmer 2400 series II CHN/S analyzer. Conductance was measured with a Hanna (HI-8633) conductivity

meter (Romania). The degree of magnetization for titanium complexes was measured on Sherwood MSB Mk1 magnetic susceptibility balance using sealed-off MnCl_2 solution as calibrant at room temperature. Chloride contents were determined volumetrically using AgNO_3 in the presence of indicator potassium chromate solution (1% w/v) [23]. Titanium content in Ti(III) hydrazide complexes was determined volumetrically by the reported method of redox reaction using standard iron(III) ammonium sulfate solution in the presence of potassium thiocyanate solution as an indicator [13].

Synthesis of hydrazide ligands

Hydrazide ligands were synthesized by reported methods by the reaction of hydrated hydrazine with respective ester. First, 50 mmol of hydrated hydrazine was added to an ethanolic solution of ester (10 mmol in 50 mL). Then, the mixture was refluxed for 2-3 h. The products were obtained from crystals separated, washed with hexane, and dried. Ligands were further purified after recrystallization from methanol by slow evaporation.

Synthesis of Ti(III) hydrazide complexes

To synthesize Ti(III) hydrazide complexes, metal and ligand were mixed in 1:2 molar ratios. Then, the methanolic solution of TiCl_3 (10 mmol in 10 mL) was slowly added to the synthesized ligands in methanol (20 mmol in 20 mL) with continuous stirring at room temperature. As a result, solid particles were obtained, which were separated and washed with methanol to remove excess reactants. Finally, the precipitates were dried in the air.

Synthesis of Ti(IV) complexes

Our research group has already published the synthesis and characterization of Ti(IV) hydrazide complexes with ligands La-Lf, Lh [24]. The synthesis and structures of Ti(IV) hydrazide complexes are shown in Scheme 1.

Enzyme inhibitory activities

Tyrosinase inhibition assay

Tyrosinase inhibition assay was performed in 96 well plate spectrophotometers described by Kim with slight modification [25]. The mixture of 60 units of enzyme, 10 μL of sample in DMSO solution, and 150 μL of buffer (50 mM of pH 6.8) in each well was incubated for 15 min at 30 °C. Then 20 μL of the substrate (L-tyrosine) per well was added and re-incubated at the same condition for 30 min. Dopachrome formed after incubation was determined at 480 nm in a microplate reader. The control comprised 10 μL of DMSO instead of the sample solution. Kojic acid was taken as a positive control for tyrosinase inhibitors. Triplicate sets were used for experiments. Tyrosinase inhibitory percentage was calculated by the formula given below:

$$\% \text{ Inhibition of tyrosinase} = \frac{(A_c - A_s) \times 100}{A_c} \quad (1)$$

where A_c is the absorbance of the control and A_s is the absorbance of the sample solution.

Lipoxygenase inhibition assay

LOX inhibition abilities of the samples were determined by the spectrophotometric method described by Tappel *et al.* with slight modifications [26]. First, the working solution of the LOX enzyme was made and adjusted up to the concentration of the enzyme, displaying the values of

0.05 absorbance/min. Next, 10 μL of test solution (in DMSO) was added to 160 μL (100 mM) of pH 8 sodium phosphate buffer, and then 20 μL of LOX solution was added. The resulting mixture was incubated at 25 $^{\circ}\text{C}$ for 10 min. After incubation, 10 μL substrate solution (linoleic acid, 0.5 mM) was used to initiate the reaction, and the reaction mixture was left for 5 min at room temperature. Then the conversion of linoleic acid to 13-hydroperoxylinoleic acid was observed, and absorbance was measured at 234 nm using a microplate reader. Finally, the inhibitory concentration of the test compound, at which 50% of the enzyme was inhibited, was determined by varying the concentrations of test compounds using the EZ-Fit Enzyme kinetics program (Perrella Scientific In., Amherst, USA).

Molecular docking

Two target proteins were retrieved from the protein data bank for docking Ti(III) and Ti(IV) hydrazide complexes. The 5-LOX enzyme 3V99 PDB [27] was used, and the tyrosinase enzyme 4UOA PDB [28] was used. Both the proteins were set up for docking by removing water molecules and hetero atoms. In the case of 4UOA protein, chain B was used for docking as it contains copper transition metal at the active site. Similarly, copper metal was retained in chain B of 4UOA. Docking was performed by the online web server PatchDock [29]. Further PLIP [30] online web tool was used to predict protein ligand-complexes interaction.

Initially, Chem draw was used to build the structure of Ti(III) and Ti(IV) complexes. For docking, the Patch Dock server was used with default parameters. For the prediction of binding pattern PLIP online web tool was used to depict protein-ligand complexes interactions. In Patch Dock, the results were evaluated based on atomic contact energy (ACE); a more negative value of ACE shows a greater affinity of the docked compound with the protein. The PLIP web tool was used to evaluate the binding pattern.

RESULTS AND DISCUSSION

Synthesis and physicochemical properties

The hydrazide ligands (**L_a**-**L_g**) were synthesized in good yields (71-85%) and characterized using spectroscopic (IR, EI-MS) and microanalytical (CHN) techniques. Ti(III) hydrazide complexes were synthesized by directly mixing the methanolic solution of TiCl_3 with methanolic hydrazide solution in 1:2 ratios at room temperature (Scheme 1, Table 1).

Dichlorobisbenzohydrazidetitanium(III) chloride (3a). Brown solid; yield: 85.52%. FTIR (KBr cm^{-1}): 1632 (C=O), 3054, 3200 (NH_2 stretch.), 3241 (NH), 1577 (NH_2 bend.), 1666 (C=C), 1485 (C-N); anal. calcd. for $\text{C}_{14}\text{H}_{16}\text{N}_4\text{O}_2\text{Cl}_3\text{Ti}$ (FW = 426.531 g mol^{-1}): C, 43.68; H, 5.14; N, 18.71; Ti, 11.15; Cl, 8.23%. Found: C, 43.56; H, 5.26; N, 18.57; Ti, 11.22; Cl, 8.31%. Molar conductivity (DMSO): Λ_{M} , 62.97 $\Omega^{-1}\text{cm}^2\text{mol}^{-1}$, μ_{eff} 1.71 B.M.

Dichlorobis(4-chlorobenzohydrazidetitanium(III) chloride (3b). White solid; yield: 85%; FTIR (KBr cm^{-1}): 1646 (C=O), 3025, 3148 (NH_2 stretch.), 3064 (NH), 1598 (NH_2 bend.), 1487 (C=C), 1342 (C-N); anal. calcd. for $\text{C}_{14}\text{H}_{14}\text{N}_4\text{O}_2\text{Cl}_5\text{Ti}$ (FW = 495.27 g mol^{-1}): C, 33.94; H, 2.85; N, 11.31; Ti, 9.66; Cl, 7.15%. Found: C, 33.87; H, 2.79; N, 11.26; Ti, 9.85; Cl, 7.18%. Molar conductivity (DMSO): Λ_{M} , 45.86 $\Omega^{-1}\text{cm}^2\text{mol}^{-1}$, μ_{eff} 1.75 B.M.

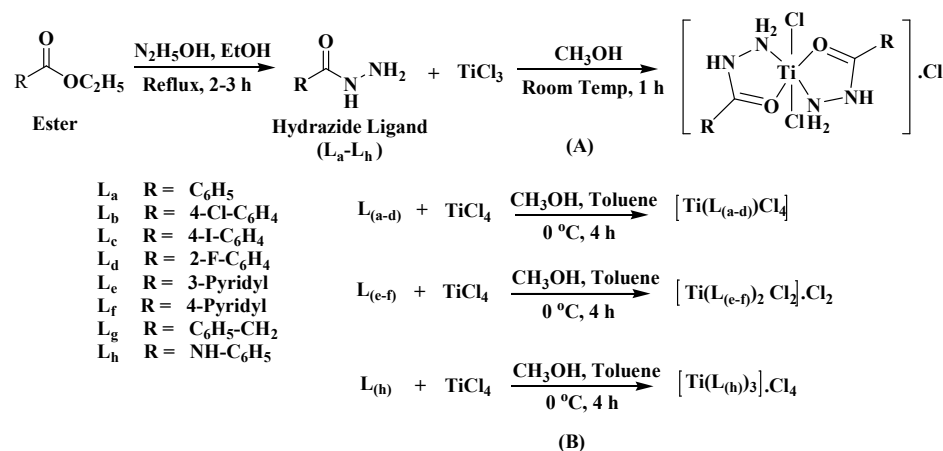
Dichlorobis(4-iodobenzohydrazidetitanium(III) chloride (3c). White solid; yield: 80%; FTIR (KBr cm^{-1}): 1640 (C=O), 3167, 3080 (NH_2 stretch.), 3066 (NH), 1603 (NH_2 bend.), 1553 (C=C), 1331 (C-N); anal. calcd. for $\text{C}_{14}\text{H}_{14}\text{N}_4\text{O}_2\text{Cl}_3\text{ITi}$ (FW = 678.33 g mol^{-1}): C, 24.78; H, 2.07; N, 8.25; Ti, 7.05; Cl, 5.22%; Found: C, 24.85; H, 2.14; N, 8.57; Ti, 7.15; Cl, 5.35%. Molar conductivity (DMSO): Λ_{M} , 65.64 $\Omega^{-1}\text{cm}^2\text{mol}^{-1}$, μ_{eff} 1.78 B.M.

Dichlorobisnicotinicbenzoyhydrazidetitanium(III) chloride (3e). Brown solid; yield: 81%; FTIR (KBr cm^{-1}): 1653 (C=O), 3130, 3210 (NH_2 stretch.), 3057 (NH), 1607 (NH_2 bend), 1563 (C=C), 1339 (C-N); anal. calcd. for $\text{C}_{12}\text{H}_{14}\text{N}_6\text{O}_2\text{Cl}_3\text{ITi}$ (FW = 428.51 g mol^{-1}): C, 33.63; H, 3.29; N, 19.61; Ti, 11.17; Cl, 8.27%; Found: C, 33.71; H, 3.26; N, 19.75; Ti, 10.95; Cl, 8.24%. Molar conductivity (DMSO): Λ_M , 35.26 $\Omega^{-1}\text{cm}^2\text{mol}^{-1}$. μ_{eff} 1.73 B.M.

Dichlorobisisonicotinicbenzoyhydrazidetitanium(III) chloride (3f). White solid; yield: 85%; FTIR (KBr cm^{-1}): 1676 (C=O), 3292, 3165 (NH_2 stretch.), 3052 (NH), 1612 (NH_2 bend.), 1577 (C=C), 1323 (C-N); anal. calcd. for $\text{C}_{12}\text{H}_{14}\text{N}_6\text{O}_2\text{Cl}_3\text{ITi}$ (FW = 428.51 g mol^{-1}): C, 33.63; H, 3.29; N, 19.61; Ti, 11.17; Cl, 8.27%; Found: C, 33.76; H, 3.36; N, 19.57; Ti, 10.95; Cl, 8.30%. Molar conductivity (DMSO): Λ_M , 59.70 $\Omega^{-1}\text{cm}^2\text{mol}^{-1}$. μ_{eff} 1.76 B.M.

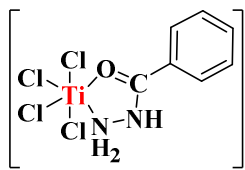
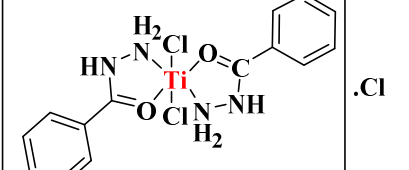
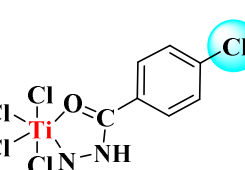
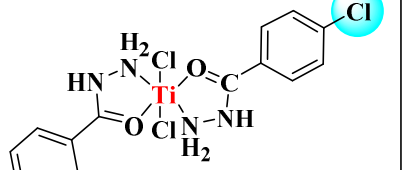
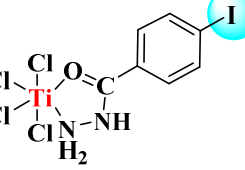
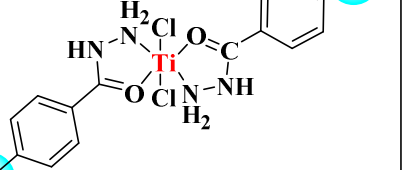
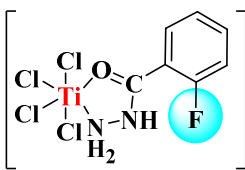
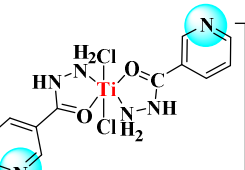
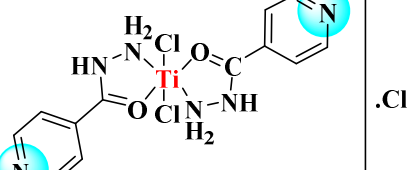
Dichlorobis2-phenylacetohydrazidetitanium(III) chloride (3g). Light brown solid; yield: 85%; FTIR (KBr cm^{-1}): 1696 (C=O), 3204, 3057 (NH_2 stretch), 3004 (NH), 1590 (NH_2 bend.), 1476 (C=C), 1358 (C-N). anal. calcd. for $\text{C}_{16}\text{H}_{20}\text{N}_4\text{O}_2\text{Cl}_3\text{Ti}$ (FW = 454.61 g mol^{-1}): C, 42.27; H, 4.43; N, 12.32; Ti, 10.53; Cl, 7.80%. Found: C, 42.23; H, 4.32; N, 12.40; Ti, 10.55; Cl, 7.75%. Molar conductivity (DMSO): Λ_M , 41.58 $\Omega^{-1}\text{cm}^2\text{mol}^{-1}$. μ_{eff} 1.72 B.M.

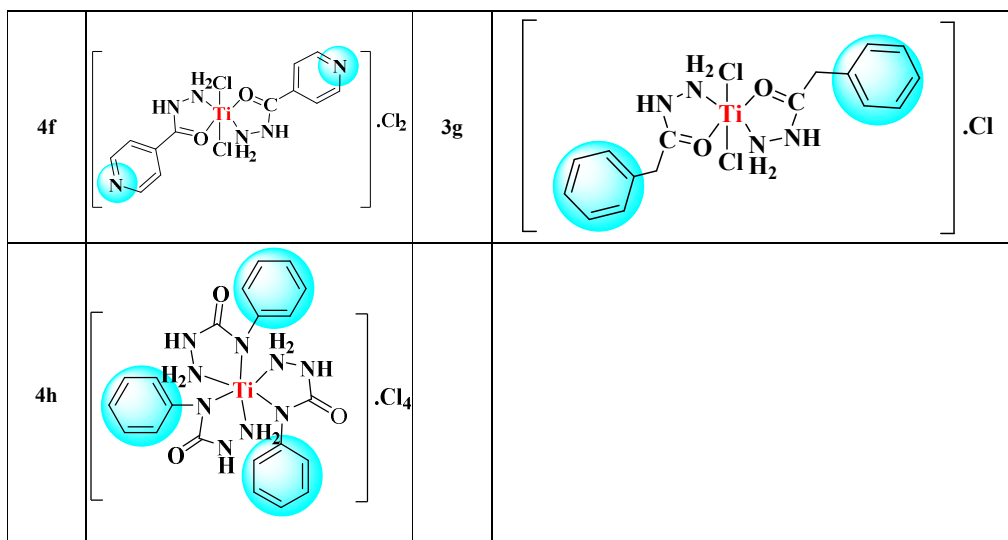
Spectral and analytical measurements were applied for the structural elucidation of synthesized complexes (**3a-3c**, **3e-3g**). The experimental section has provided elemental, physical, and analytical data on complexes. Based on the obtained results, the Ti(III) complexes are tentatively assigned to exhibit octahedral geometry displaying the bidentate coordination of ligands to metal. The molar conductivity of Ti(III) complexes in DMSO was 35.26–65.64 $\Omega^{-1}\text{cm}^2\text{mol}^{-1}$. The values gave the idea of the electrolytic nature of complexes. Molar conductivity values indicate a 1:1 electrolytic ratio of coordination sphere to chloride ion outside the sphere [31]. Complexes were found to be non-hygroscopic and brown in color and showed good solubility in organic solvents like DMSO and DMF. The effective magnetic moments (μ_{eff}) of Ti(III) complexes, in the range of 1.71 to 1.78 B.M. suggested the paramagnetic nature of titanium complexes. This value also confirmed the d^1 system and the octahedral geometry of complexes as previously reported for Ti(III) complexes (d^1 system) [32, 33]. Despite being oxidation sensitive, Ti(III) did not oxidize to Ti(IV) during complexation, as evident from the obtained spin value.



Scheme 1. Synthesis of (A) Ti(III), and (B) Ti(IV) hydrazide complexes.

Table 1. Structures of synthetic Ti(III) and Ti(IV) hydrazide complexes.

Compd.	Structures (Ti(IV) complexes)	Compd.	Structures (Ti(III) complexes)
4a		3a	
4b		3b	
4c		3c	
4d		3e	
4e		3f	



Spectroscopic analysis

The hydrazide ligands are known to possess two coordination sites, i.e. carbonyl oxygen and amino nitrogen. The binding mode of the hydrazide ligands to Ti(III) in the newly synthesized complexes was evaluated by the exhaustive comparison study of the IR spectra of the ligands with the spectra of Ti(III) complexes. IR spectra of Ti(III) complexes suggest the neutral bidentate coordination of ligands using carbonyl oxygen and hydrazinyl nitrogen.

The sharp peak of C=O absorption at $1652 \pm 22 \text{ cm}^{-1}$ in ligands shifted to considerable frequency ($1668 \pm 28 \text{ cm}^{-1}$) upon complexation, indicating carbonyl oxygen's involvement in coordination with the metal center. In all complexes, the C=O band shifted to a higher frequency while the C-N band shifted to a lower frequency. The positive frequency shift suggests a decrease in the double bond character of C=O and an increase in the double bond character of C-N, which is supported by the negative shift in C-N frequency [34].

A doublet band around $3030\text{-}3322 \text{ cm}^{-1}$ is characteristic of the N-H stretching frequency of the hydrazinyl group. Significant broadening of this band with a lowering of frequency was observed in the spectra upon complexation with Ti(III) center. It supports the coordination of primary nitrogen with the Ti(III) metal center. The bands of benzene skeleton (C=C stretching), NH_2 bending, and NH stretching are also identified in the spectra of ligands and complexes.

UV-visible electronic transitions of freshly prepared solution of hydrazide (**L_a**-**L_c**, **L_c**-**L_g**) and their Ti(III) complexes (**3a-3c**, **3e-3g**) were observed in DMSO. For comparative purposes, electronic transitions of ligands were also listed. The paramagnetic titanium(III) chloride has a d^1 system with ${}^2T_{2g}$ ground state and 2E_g as spin-allowed transitions state. The electronic spectrum of titanium(III) chloride in DMSO showed a prominent band at 525 nm with a shoulder around 575 nm. These transitions are assigned from ${}^2T_{2g}$ to ${}^2B_{1g}$ and ${}^2A_{1g}$, respectively. All Ti(III) complexes showed one broadband assigned to ${}^2T_{2g}$ to 2E_g with slight shifting in the range of 495-518 nm. The presence of this band confirms the octahedral geometry of complexes [4, 35]. Molar absorptivity values ($42\text{-}73 \text{ M}^{-1}\text{cm}^{-1}$) suggested this transition as Laporte forbidden, spin allowed. All ligands exhibit π to π^* transition, which comes from the aromatic ring of hydrazide. Upon coordination with Ti(III), these transitions slightly shifted to a lower wavelength which is a sign of lowering the π -orbital energy of the hydrazide ligand.

Based on IR and elemental data, Ti(III) hydrazide complexes are proposed to possess octahedral geometry with neutral hydrazide ligands. The bidentate coordination of ligands was found to have occurred through the oxygen of the carbonyl group and primary amine nitrogen. Ti(IV) hydrazide complexes were also reported to possess octahedral geometries in which the hydrazide ligands are coordinated by the primary amine nitrogen and carbonyl oxygen donor atoms for complexes **4a-4f**. In contrast, the imino nitrogen is coordinated in complex **4h** [24].

Cytotoxic activities of Ti(III) and Ti(IV) hydrazide complexes

Cytotoxic activity of all Ti(III) and Ti(IV) complexes (100 μM) on normal 3T3 cells have been measured by the appearance of purple color after reduction of MTT (3-(4,5-dimethylthiazol-2-yl)-2,5-diphenyltetrazolium bromide) to formazan. Cyclohexamide was used as a standard inhibitor of cytotoxic activity. Most of the complexes found inactive, except **4b**, **4c**, and **3c** showed cytotoxicity much less than standard cyclohexamide. In addition, the precursor metal solutions, TiCl_4 and TiCl_3 , were also found to be non-cytotoxic against normal cells.

Amongst Ti(IV) hydrazide complexes **4a-4h**, *para*-chloro substituted Ti(IV) complex **4b** ($\text{IC}_{50} = 30.4 \pm 1.2 \mu\text{M}$) was found to be very weakly cytotoxic as compared to standard cyclohexamide ($\text{IC}_{50} = 0.3 \mu\text{M}$). Replacing chloro with iodo in the case of complex **4c** ($\text{IC}_{50} = 27.7 \pm 0.4 \mu\text{M}$) showed almost the same cytotoxicity as **4b**. Similarly, *para*-iodo substituted Ti(III) complex **3c** ($\text{IC}_{50} = 23.3 \pm 1.5 \mu\text{M}$) showed slightly enhanced activity than structurally similar Ti(IV) complex **4c**.

Tyrosinase inhibitory activity

Tyrosinase enzyme has a strongly coupled binuclear copper center. It is proposed that inhibitors interact with that binuclear center in the enzyme's active site. Four types of inhibitors can be seen based on their mode of interaction with the enzyme. Inhibitors that compete with substrate and combine directly with free enzymes are competitive inhibitors. Uncompetitive is the one that combines only to enzyme-substrate complex, and the inhibitors bind to both. The enzyme or enzyme-substrate complex with the same and different equilibrium constants are non-competitive and mixed-type inhibitors. Most hydrazides are reported to exhibit mixed-type inhibition [36].

The inhibition potential for all hydrazide ligands and their Ti complexes against tyrosinase enzyme has been investigated by measuring the low absorbance of dopachrome at 480 nm using an L-tyrosine oxidation assay. Kojic acid was taken as the standard tyrosinase inhibitor ($\text{IC}_{50} = 25 \pm 0.4 \mu\text{M}$). The free hydrazide ligands and Ti metal are inactive, while their Ti(IV) hydrazide complexes displayed IC_{50} values in the range of 4.7 to 151 μM compared to the standard. Specifically, complex **4d** displayed enzyme activation. Carbonyl hydrazide moiety could form a complex with the active site copper center of tyrosinase enzyme, thus taking an important part in inhibition [17, 37, 38]. Four out of six Ti(IV) complexes, including **4a**, **4e**, **4f**, and **4h**, showed the most potent inhibitors of tyrosinase enzyme in comparison to the standard Kojic acid. An unsubstituted **4a** ($\text{IC}_{50} = 4.7 \pm 0.3 \mu\text{M}$) complex with only a benzene ring of hydrazide ligand was the most potent inhibitor and five-fold more active than the standard. Incorporation of halides *e.g.* Cl and I at *para* positions of benzene ring in cases of **4b** ($\text{IC}_{50} = 140.0 \pm 0.2 \mu\text{M}$) and **4c** ($\text{IC}_{50} = 151.0 \pm 0.4 \mu\text{M}$) lead to steep decline in the inhibitory potential (Figure 1).

However, Ti complex **4d** having *ortho*-fluoro substitution at the benzene ring exhibits a negative inhibition value showing the enzyme activating property. For effectors binding, an effector site is also present in the tyrosinase enzyme in addition to the active site [39]. As reported for sodium dodecyl sulfate (SDS), limited conformational change in latent enzyme after binding to SDS is related to the activation process [40-42]. Fatty acid produces conformational change and hence showed activation of tyrosinase enzyme. Since fluoro-carbon compounds are hydrophobic [43], in our research, it can be proposed that the hydrophobic fluoro-carbon can bind

to the effect or site of the enzyme with a strong hydrophobic attraction leading the conformational change in the active site of the enzyme. This conformational change makes the active site more effective than the substrate, resulting in activation (Figure 1).

Pyridyl ring bearing Ti(IV) complexes **4e** ($IC_{50} = 5.8 \pm 0.5 \mu M$) and **4f** ($IC_{50} = 7.9 \pm 0.4 \mu M$) demonstrated potent inhibitory potential against tyrosinase enzyme. Studies revealed that replacing the benzene ring with an electron-rich aromatic moiety favors the binding of the inhibitor with the active site of the enzyme resulting in better inhibition potential [40]. Recent studies also described the role of pyridyl nitrogen of inhibitors in the complex formation with the copper center in the enzyme's active site [44, 45]. Minor difference in results indicates the positional effect of pyridyl N of a benzene ring on inhibition. Complex **4h** ($IC_{50} = 5.4 \pm 0.3 \mu M$) possesses the second most potent activity among all the complexes (Figure 1). The hydrazide ligand contains an imino N in addition to the hydrazinyl N, thus forming the electron-rich complex which favors the inhibition potential. The Ti complex (**4h**) is most symmetric in structure as the Ti center is coordinated to three same bidentate ligands giving perfect O_h geometry. The symmetric structure may also be the reason for the high potency since the significant effect of molecular symmetry on enzyme inhibition is already reported [46].

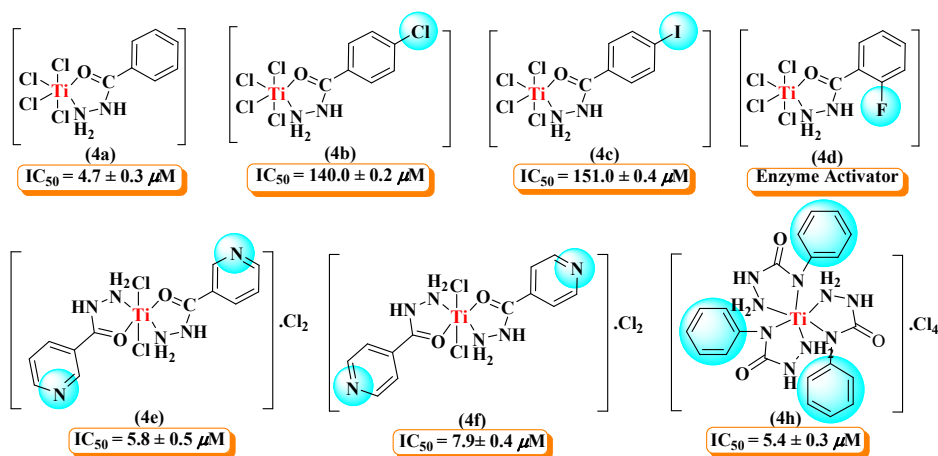


Figure 1. Tyrosinase inhibitory activities of Ti(IV) hydrazide complexes **4a-4f**, **4h**.

$TiCl_3$ itself is found to be inactive, while the complexes are found to be active against tyrosinase enzyme. Ti(III) hydrazide complexes exhibited varying degrees of tyrosinase inhibition displaying the same activity trend as discussed for Ti(IV) hydrazide complexes. The simplest unsubstituted complex **3a** ($IC_{50} = 5.6 \pm 0.3 \mu M$) is found to be the most potent amongst all complexes, while the substitution of halo groups, i.e. chloro in **3b** ($IC_{50} = 160.0 \pm 0.4 \mu M$) and iodo in **3c** ($IC_{50} = 178.0 \pm 0.2 \mu M$) at the *para* position of the benzene ring, decreased the activity of complexes and exhibited weak inhibition. Pyridyl ring complexes, **3e** ($IC_{50} = 7.8 \pm 0.5 \mu M$) and **3f** ($IC_{50} = 18.0 \pm 0.3 \mu M$) displayed increased inhibition potential exhibiting IC_{50} values (7.8 and 18 μM , respectively) better than the standard Kojic acid. The electron-donating groups are reported to exhibit more potency than halogen substitution on the benzene ring [47]. Complex **3g** ($IC_{50} = 63.0 \pm 0.4 \mu M$), with residual methylene ($-CH_2$) in between the carbonyl group and benzene ring of ligand, displayed good inhibition, suggesting the effective involvement of the CH_2 group in enhancing the inhibitory potential against tyrosinase enzyme (Figure 2).

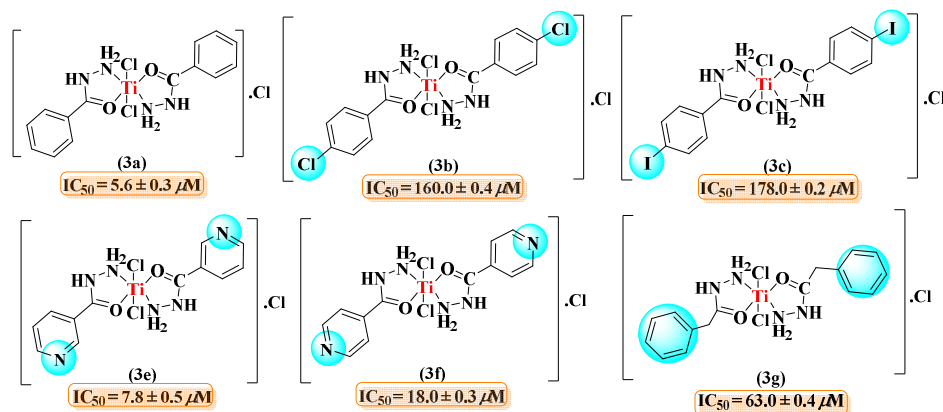


Figure 2. Tyrosinase inhibitory activities of Ti(III) hydrazide complexes **3a-3c**, **3e-3g**.

Docking analysis

The docking analysis confirms that hydrazide compounds are inactive against the tyrosinase enzyme and do not bind at the active site of the tyrosinase enzyme. Figure 3 shows that all hydrazide ligands have similar binding patterns with His4 and His5 amino acid residues but not lying at active sites and have very low ACE scores compared to complexes of hydrazide. The results validate that hydrazide compounds are not binding at the binding pocket and are inactive against the tyrosinase enzyme's experimental activity. However, the estimation of the binding mechanism of Ti(III) and Ti(IV) complexes results in a variable degree of docking binding energies. In the case of Ti(III) complexes (Figure 4), the most potent complex is **3a** and **3e** for tyrosinase enzyme, where docking results also show the highest binding affinity with this complex at the active site owing -235.56 cal/mol and -224.5 cal/mol, respectively. They form a hydrogen bond with GLN294 at a distance of 1.98 Å and 3.14 Å. In addition, complex **3e** also forms a hydrogen bond with SER291 and GLY299 at a distance of 3.06 Å and 2.78 Å, respectively. In the case of complex **3f**, binding energies follow a similar pattern with experimental activities and form hydrogen bonds, including SER291, GLN294, GLY299, THR343, ASP344, THR345, ALA346, and SER351 at a distance of 3.43, 2.24, 3.14, 3.16, 2.56, 2.15, 3.20, and 2.57 Å, respectively. Complex **3g** has binding energy -183.79 cal/mol mediating hydrogen bond with GLN 294 at a distance of 3.48 Å, and it also forms water bridge interaction with ALA346 at a distance of 3.76 Å. Complexes **3b** and **3c** have low experimental activity and mediate weak hydrogen bonds with SER439 and GLN294, respectively. In the case of Ti(IV) complexes (Figure 4), compounds **4a**, **4h**, **4e**, and **4f** show high experimental activity and good binding affinity with active site amino acid residues, including LYS66, THR70, GLN294, THR343, ASP345, ARG376. In addition, complex **4h** also mediates polar contact with surrounding water molecules by making a water bridge with ALA346 at a distance of 3.06 Å. It also has π -stacking interactions with PHE355. Complexes **4b** and **4c** have low experimental activity, so compound **4b** does not interact with surrounding amino acids, whereas compound **4c** only forms a bond with THR70 at a distance of 2.18 Å. Complex **4d** acts as an experimental activity activator and forms bonds with SER 291 at a distance of 2.79 Å.

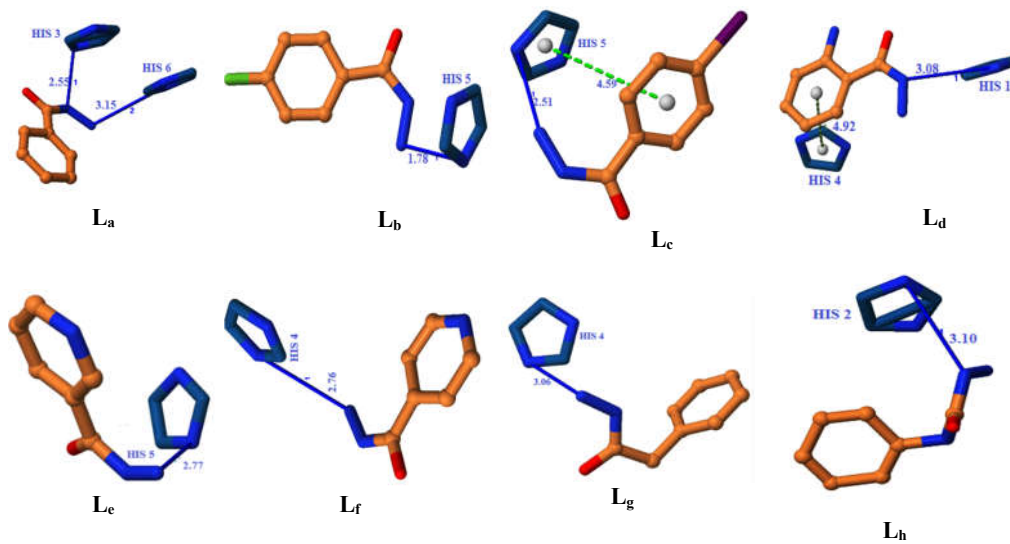
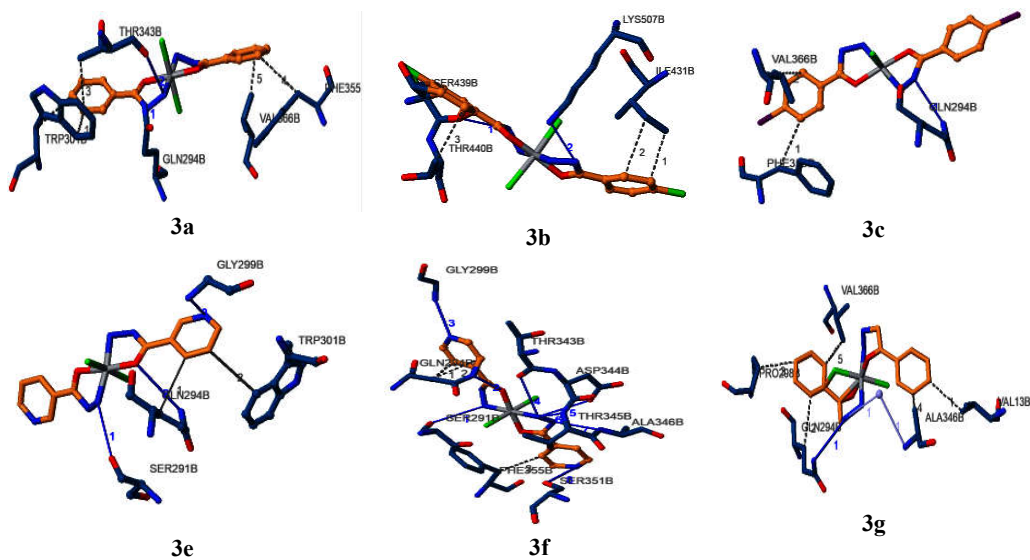


Figure 3. Binding interactions of hydrazone ligands with tyrosinase enzyme



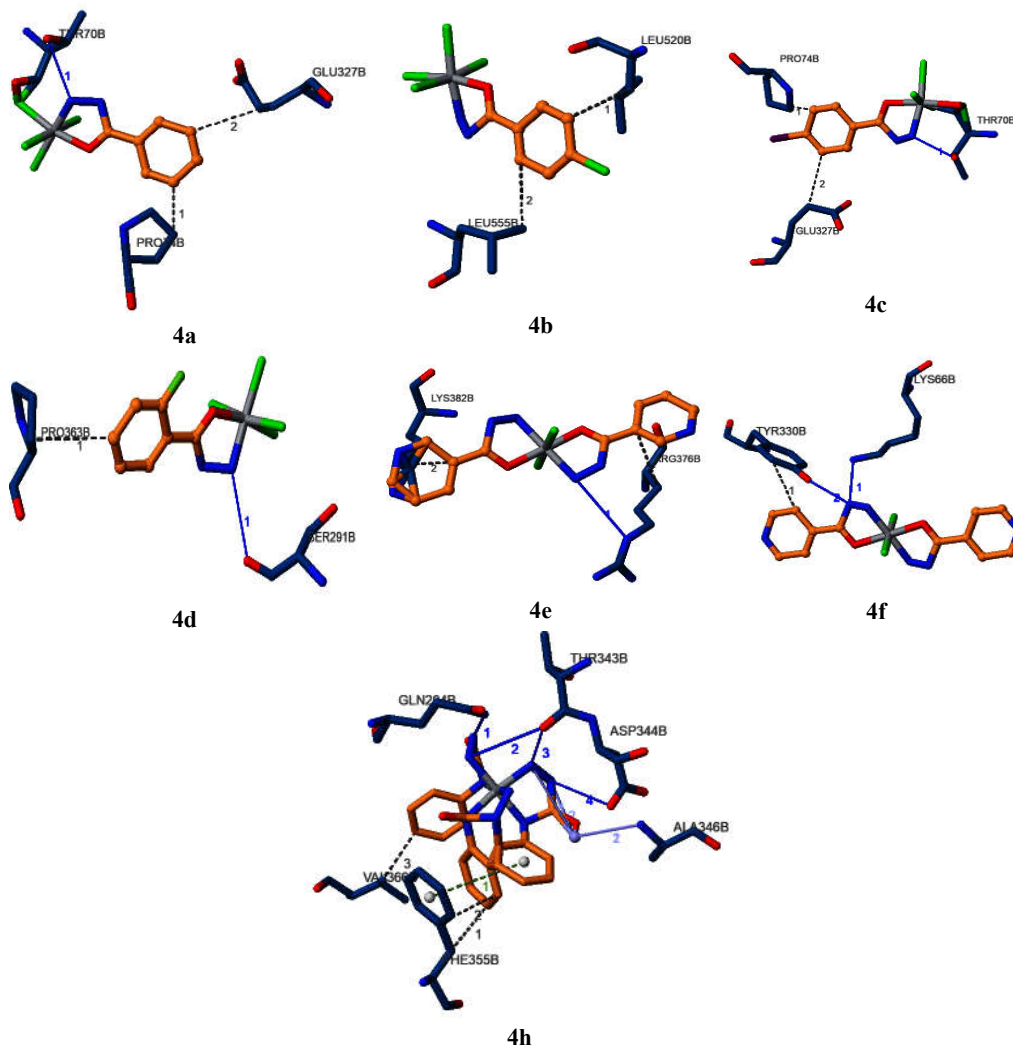


Figure 4. Binding interactions of Ti(III) and Ti(IV) hydrazone complexes with tyrosinase active site.

Lipoxygenase inhibitory activities

The inhibition potential of the hydrazides, their Ti(III) and (IV) complexes, and precursor metal solutions (TiCl_3 and TiCl_4), have been screened for lipoxygenase inhibition activity. All the hydrazides and their respective titanium complexes showed varying degrees of LOX inhibition, while the metal solutions (TiCl_3 and TiCl_4) possess no activity. Baicalein was the standard lipoxygenase inhibitor with an IC_{50} value of $27 \pm 0.4 \mu\text{M}$.

The non-coordinated hydrazides exhibited superior LOX inhibition in the range of 28-55 μM compared to the metal complexes and standard inhibitor. It may be due to the ability of the ligand

to coordinate with the active site of the enzyme, Fe^{+3} , and reduce it to the inactive Fe^{+2} [48, 49]. The hydrazide **L_e** ($\text{IC}_{50} = 28 \pm 0.3 \mu\text{M}$) with unsubstituted benzyl ring is the most potent inhibitor among all the hydrazides compared to the standard. The substitution of halide groups decreases the inhibition activity of ligands depending upon the nature and position of the substituent. *para*-chloro and *para*-iodo bearing ligands **L_b** ($\text{IC}_{50} = 45 \pm 0.4 \mu\text{M}$) and **L_c** ($\text{IC}_{50} = 40 \pm 0.3 \mu\text{M}$) displayed comparatively better activity in comparison to *ortho*-fluoro substituted **L_d** ($\text{IC}_{50} = 55 \pm 0.2 \mu\text{M}$). Replacement of benzene ring with 3-pyridyl **L_e** ($\text{IC}_{50} = 28 \pm 0.3 \mu\text{M}$) and 4-pyridyl **L_f** ($\text{IC}_{50} = 29 \pm 0.5 \mu\text{M}$) ligands display no change in the LOX inhibition activity having results similar to benzyl ring hydrazide. Imino moiety in between the carbonyl group and benzene ring of hydrazide ligand **L_h** ($\text{IC}_{50} = 40 \pm 0.5 \mu\text{M}$) positively affects inhibition activity. The presence of the CH_2 group in between carbonyl and benzene ring in hydrazide ligand **L_g** ($\text{IC}_{50} = 47 \pm 0.6 \mu\text{M}$) results in a lowering of LOX inhibition activity.

Ti(IV) hydrazide complexes exhibited moderate LOX inhibitory activity in the range of $\text{IC}_{50} = 58$ to $99 \mu\text{M}$. The presence of titanium metal may hinder the coordination of hydrazide with iron situated at the active site of lipoxygenase, thus lowering the activity of complexes compared to the free hydrazide ligands. The pyridyl ring complexes **4e** ($\text{IC}_{50} = 58 \pm 0.5 \mu\text{M}$) and **4f** ($\text{IC}_{50} = 60 \pm 0.6 \mu\text{M}$) possess the noteworthy inhibition potential amongst all Ti(IV) complexes. Complex **4h** ($\text{IC}_{50} = 63 \pm 0.3 \mu\text{M}$) with imino moiety in between the carbonyl group and benzene ring also displayed imperious LOX inhibiting activity. The results suggest nitrogen moiety's operative role in enhancing the LOX inhibition potential of Ti(IV) hydrazide complexes **4e**, **4f**, and **4h**. It is worth mentioning that the same complexes possess efficient antioxidative properties against DPPH. Since the compounds possessing DPPH scavenging potential exhibit remarkable antiinflammatory and antiaging properties [50]. Unsubstituted **4a** ($\text{IC}_{50} = 88 \pm 0.3 \mu\text{M}$), *para*-chloro **4b** ($\text{IC}_{50} = 99 \pm 0.2 \mu\text{M}$), *para*-iodo **4c** ($\text{IC}_{50} = 85 \pm 0.2 \mu\text{M}$), and *ortho*-fluoro **4d** ($\text{IC}_{50} = 87 \pm 0.4 \mu\text{M}$) hydrazide complexes demonstrated moderate and closed inhibitory activities (Figure 5).

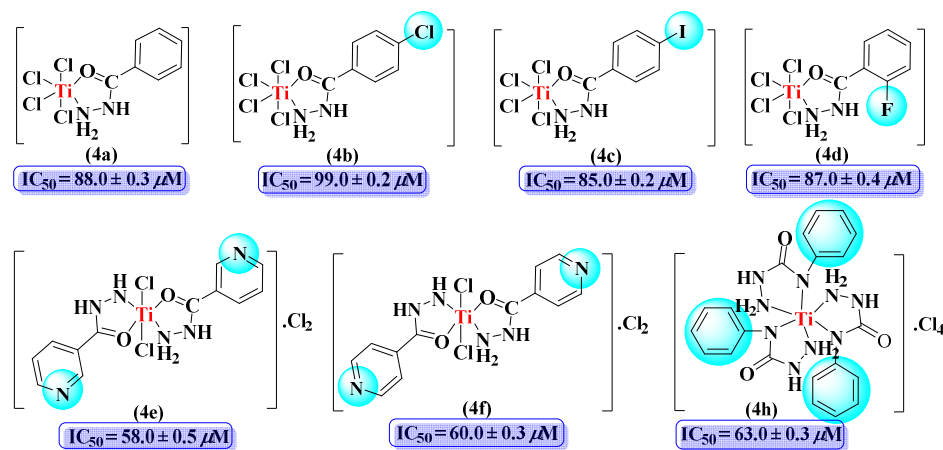


Figure 5. LOX inhibitory activities of Ti(IV) hydrazide complexes **4a-4f**, **4h**.

LOX inhibition activity of Ti(III) hydrazide complexes was found in the range of $57 - 89 \mu\text{M}$, lower than hydrazide ligands. Complex **3g**, with the CH_2 group in between $\text{C}=\text{O}$ and benzene ring, displayed no inhibition activity against the LOX enzyme, while the respective free ligand exhibited good activity. The low activity in the case of complexes supports our hypothesis that the coordination of hydrazide and active site iron is hindered in the presence of Ti(III) metal. The

complex with unsubstituted benzene ring **3a** ($IC_{50} = 79 \pm 0.4 \mu M$) showed moderate inhibitory potential than the standard baicalein ($IC_{50} = 27 \pm 0.4 \mu M$). The increase in activity was observed after the substitution of the iodo group at *para* position **3c** ($IC_{50} = 57 \pm 0.6 \mu M$) while replacing iodo with the chloro group in the case of complex **3b** ($IC_{50} = 89 \pm 0.5 \mu M$) resulted in decreased inhibitory potential. The pyridyl bearing complexes **3e** ($IC_{50} = 74 \pm 0.2 \mu M$) and **3f** ($IC_{50} = 69 \pm 0.4 \mu M$) also displayed moderate activities. No marked effect was observed with respect to the position of pyridyl nitrogen (Figure 6).

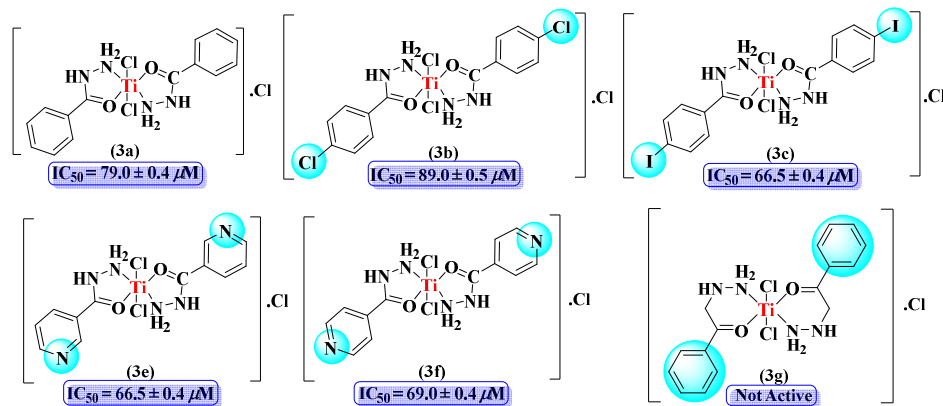
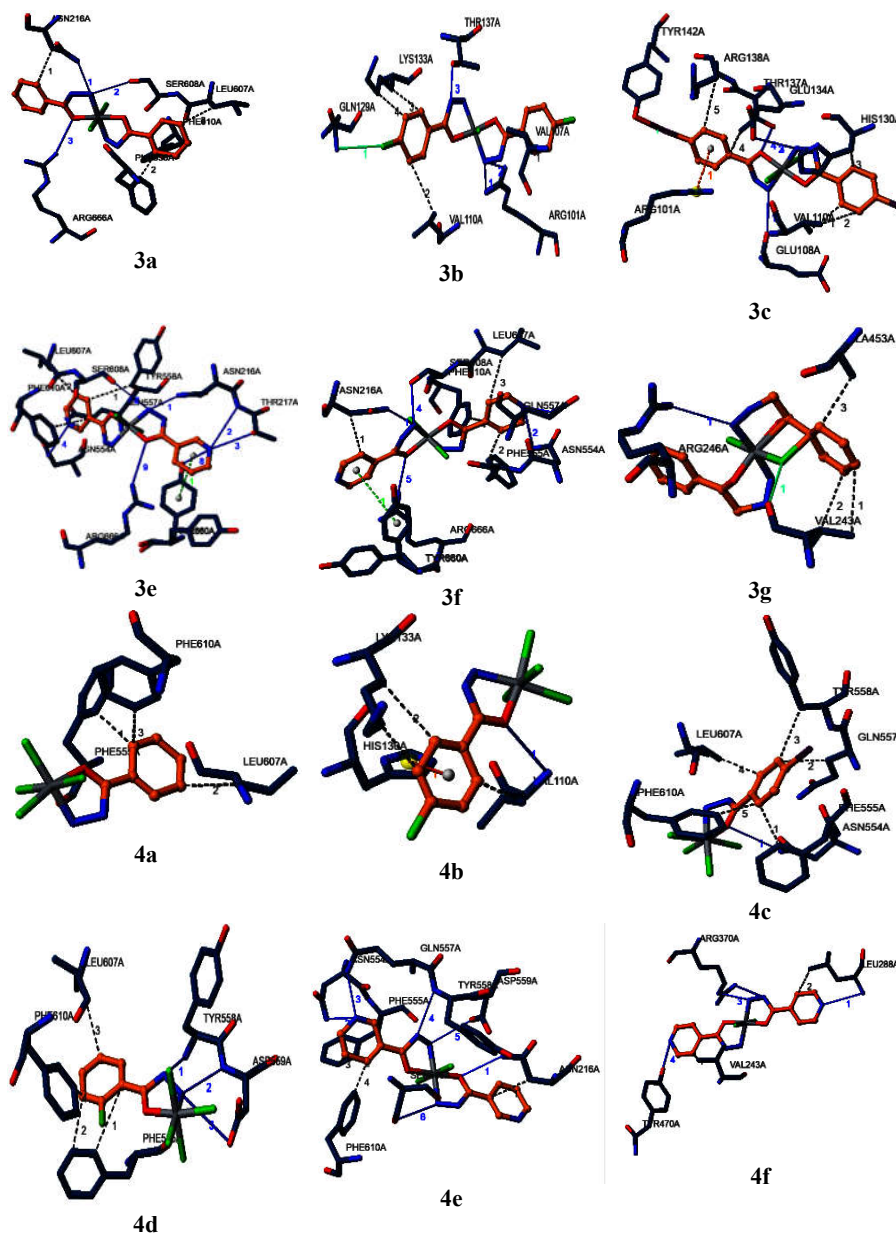


Figure 6. LOX inhibitory activities of Ti(III) hydrazone complexes **3a-3c**, **3e-3g**.

Docking studies

Docking binding patterns of hydrazides are already reported by our research group [22], while their Ti(III) and Ti(IV) complexes have been estimated for docking binding energies. In case of Ti(III) complexes (Figure 7), the most potent compound, **3c**, shows binding energy of -171.41 cal/mol. It forms two hydrogen bonds with GLU108 and GLU134 at a distance of 2.28 and 3.32 Å. In addition, it also forms a halogen bond with TYR142 at a distance of 2.42 Å and mediates π -cation interactions with ARG101. In the case of compounds, **3a** and **3e** binding energies follow a similar pattern with experimental activities, and both **3a** and **3e** form bonds with ASN216, SER608, and ARG666. In the case of compound **3b**, experimental activity is low among all compounds, and it also has low binding energy, *i.e.*, -156.18 cal/mol as compared to other compounds, and only forms bonds with ARG 101 and THR137. For compound **3g**, lipoxygenase activity is nil, so docking energy is very low, *i.e.* -83.31 cal/mol. For compounds **4e** and **4h**, lipoxygenase activity is high, *i.e.* 58 μM and 63 μM , respectively (Figure 7), so binding energies are also higher, *i.e.* -197.99 and -189.13 cal/mol. In the case of compounds **4a**, **4c** and **4d**, experimental activity is 85-89 μM . Compound **4a** only shows hydrophobic interactions where compound **4c** forms a hydrogen bond with ASN554 at a distance of 2.46 Å. For compound **4d**, it forms a hydrogen bond with TYR558 and ASP559 at a distance of 3.13 and 3.10 Å. Compound **4b** has low experimental activity and low binding energy and only forms a bond with VAL 110 at 3.28 Å. The current findings suggested that hydrazone complexes of Ti(III) and Ti(IV) bind effectively with the target enzyme, and this study further can be used for therapeutic targets.



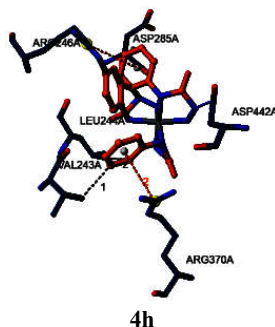


Figure 7. Binding interactions of Ti(III) and Ti(IV) hydrazide complexes against lipoxygenase enzyme.

CONCLUSION

Hydrazide ligands and their Ti(III) and Ti(IV) complexes were synthesized and characterized through chemical and physical measurements. Enzyme inhibition investigation of free hydrazide ligands and their respective Ti(III) and Ti(IV) complexes displayed a varying degree of tyrosinase and lipoxygenase inhibitory potential. The free hydrazides showed potent LOX inhibitory activity compared to the respective titanium complexes. Most of the titanium complexes exhibited good inhibitory potential against tyrosinase enzyme and hence can be used for hyperpigmentation problems, while compound **4d** is an enzyme activator. All Ti-hydrazide complexes are found non-cytotoxic against normal 3T3 cells. The foregoing activity trail of Ti-complexes suggested that the substituent modifications in the structure of hydrazide can help to explore the novel leads for antiinflammatory activity and treat melanin disorders. The non-toxic behavior of Ti(III) and Ti(IV) complexes to normal 3T3 cells also encourages the detailed study of novel titanium-based anticancer drugs against human cancer cells.

ACKNOWLEDGMENTS

Z. Shaikh is thankful to the Higher Education Commission for Indigenous Scholarship No. 213-65456-2PS2-101 under Ph.D. Fellowships for 5000 scholars, HEC (Phase-II). Furthermore, the authors thank the Higher Education Commission of Pakistan for financial support ('The National Research Grants Program for Universities', Grant No. 1862/R&D/10).

REFERENCES

1. Akhter, P.; Ashiq, U.; Jamal, R.A.; Shaikh, Z.; Mahroof-Tahir, M.; Lateef, M.; Badar, R. Chemistry, α -glucosidase, and radical scavenging properties of uranyl(VI) hydrazide complexes. *J. Med. Chem.* **2019**, *15*, 923-936.
2. Hosseini-Monfared, H.; Asghari-Lalami, N.; Pazio, A.; Wozniak, K.; Janiak, C. Dinuclear vanadium, copper, manganese and titanium complexes containing *O,O,N*-dichelating ligands: Synthesis, crystal structure and catalytic activity. *Inorg. Chim. Acta* **2013**, *406*, 241-250.
3. Taberner, V.; Cuenca, T.; Herdtweck, E. Hydrazonide titanium derivatives: Synthesis, characterization and catalytic activity in olefin polymerization. Molecular structure of [Ti(η^5 -C₅H₄SiMe₃)Cl(μ -N₂CPh₂)₂]. *J. Organomet. Chem.* **2002**, *663*, 173-182.

4. Yaul, S.R.; Yaul, A.R.; Pethe, G.B.; Aswar, A.S. Synthesis and characterization of transition metal complexes with *N,O*-chelating hydrazone Schiff base ligand. *Am.-Eurasian J. Sci. Res.* **2009**, *4*, 229-234.
5. Keller, H.; Keppler, B.; Schmähl, D. Antitumor activity of *cis*-dihalogenobis (1-phenyl-1,3-butanedionato) titanium(IV) compounds against Walker 256 carcinosarcoma. A new class of antineoplastic agents. *Arzneim. Forsch.* **1981**, *32*, 806-807.
6. Friedrich, M.; Villena-Heinsen, C.; Farnhammer, C.; Schmidt, W. Effects of vinorelbine and titanocene dichloride on human tumor xenografts in nude mice. *Eur. J. Gynaecol. Oncol.* **1997**, *19*, 333-337.
7. Peri, D.; Maker, S.; Shavit, M.; Tshuva, E.Y. Synthesis, characterization, cytotoxicity, and hydrolytic behavior of C2-and C1-symmetrical Ti(IV) complexes of tetradentate diamine bis(phenolate) ligands: A new class of antitumor agents. *Chem. Eur. J.* **2009**, *15*, 2403-2415.
8. Tzuberly, A.; Tshuva, E.Y. Cytotoxicity and hydrolysis of *trans*-Ti(IV) complexes of salen ligands: Structure-activity relationship studies. *Inorg Chem.* **2011**, *51*, 1796-1804.
9. Kaushal, R.; Thakur, A.; Bhatia, A.; Arora, S.; Nehra, K. Synthesis, characterization, DNA-binding and biological studies of novel titanium(IV) complexes. *J. Chem. Sci.* **2020**, *132*, 1-17.
10. Liu, J.J.; Fisher, D.E. Lighting a path to pigmentation: mechanisms of MITF induction by UV^A. *Pigment Cell Melanoma Res.* **2010**, *23*, 741-745.
11. Lindquist, N.G. Accumulation of drug in melanin, *Acta Radiol. Diag. (Stockh.)* **1973**, *325*, 1-92.
12. Hearing, V.J. Biogenesis of pigment granules: A sensitive way to regulate melanocyte function. *J. Dermatol. Sci.* **2005**, *37*, 13-14.
13. Kim, Y.S.; Kim, B.M.; Park, S.C.; Jeong, H.J.; Chang, I.S. A novel volumetric method for the quantitation of titanium dioxide in cosmetics. *J. Soc. Cosmet. Sci. Korea* **2005**, *31*, 289-293.
14. Peng, Z.; Wang, G.; Zeng, Q.H.; Li, Y.; Wu, Y.; Liu, H.; Wan, J.; Zhao, Y. Synthesis, antioxidant and anti-tyrosinase activity of 1,2,4-triazole hydrazones as anti-browning agents. *Food Chem.* **2021**, *341*, 128265.
15. Ghanem, G.; Fabrice, J. Tyrosinase related protein 1 melanoma. *Mol. Oncol.* **2011**, *5*, 150-155.
16. Yuan, Y.; Jin, W.; Nazir, Y.; Fercher, C.; Blaskovich, M.A.; Cooper, M.A.; Barnard, R.T.; Ziora, Z.M. Tyrosinase inhibitors as potential antibacterial agents. *Eur. J. Med. Chem.* **2020**, *187*, 111892.
17. Ferreira, S.M.; Pires, D.A.T.; Figueroa-Villar, José D. Evaluation of tetraketones and xanthenediones as tyrosinase inhibitors or activators. *J. Pharm. Pharm. Sci.* **2015**, *4*, 1705-1718.
18. Ubeid, A.A.; Hantash, B.M. Novel pentapeptide activators of mammalian and mushroom tyrosinase. *Curr. Top. Med. Chem.* **2014**, *14*, 1463-1468.
19. Skrzypczak-Jankun, E.; Zhou, K.; McCabe, N.P.; Selman, S.H.; Jankun, J. Structure of curcumin in complex with lipoxygenase and its significance in cancer. *Int. J. Mol. Med.* **2003**, *12*, 17-24.
20. Kelavkar, U.P.; Cohen, C.; Kamitani, H.; Eling, T.E.; Badr, K.F. Concordant induction of 15-lipoxygenase-1 and mutant p53 expression in human prostate adenocarcinoma: Correlation with Gleason staging. *Carcinogenesis.* **2000**, *21*, 1777-1787.
21. Zhu, J.; Kilty, I.; Granger, H.; Gamble, E.; Qiu, Y.S.; Hattotuwa, K.; Elston, W.; Liu, W.L.; Oliva, A.; Kips, J.C.; Pauwels, R.A. Gene expression and immunolocalization of 15-lipoxygenase isozymes in the airway mucosa of smokers with chronic bronchitis. *Am. J. Respir. Cell. Mol. Biol.* **2002**, *27*, 666-677.
22. Badar, R.; Ashiq, U.; Jamal, R.A.; Akhter, P.; Mahroof-Tahir, M.; Gul, S.; Ali, S.T. *In vitro* synthesis, structure elucidation and its antioxidant properties of platinum(IV)-hydrazide

- complexes: Molecular modeling of free-hydrazides suggested as potent lipoxygenase inhibitor. *Med. Chem.* **2022**, 18, 97-114.
23. Jeffery, G.H.; Bassett, J.; Mendham, J.; Denney, R.C. *Vogel's A Textbook of Quantitative Analysis*, 5th ed., Longman Scientific and Technical Ltd.: Harlow; **1963**; p 351.
 24. Shaikh, Z.; Ashiq, U.; Jamal, R.A.; Mahroof-Tahir, M.; Shamshad, B.; Sultan, S. Chemistry and antioxidant properties of titanium(IV) complexes. *Transit. Metal Chem.* **2015**, 40, 665-671.
 25. Kim, Y. Antimelanogenic and antioxidant properties of gallic acid. *Biol. Pharm. Bull.* **2007**, 30, 1052-1055.
 26. Tappel, A.L. The mechanism of the oxidation of unsaturated fatty acids catalyzed by hematin compounds. *Arch. Biochem. Biophys.* **1953**, 44, 378-395.
 27. Protein data bank, S663D Stable-5-LOX in complex with arachidonic acid, available at <http://www.rcsb.org/structure/3V99>.
 28. Protein data bank, Coexistent single-crystal structure of latent and active mushroom tyrosinase (abPPO4) mediated by a hexatungstotellurate(VI), available at <https://www.rcsb.org/3d-view/4OUA/2>.
 29. PatchDock, Molecular docking algorithm based on shape complementarity principles, available at <https://bioinfo3d.cs.tau.ac.il/PatchDock/php.php>.
 30. Protein-ligand interaction profiler, Easy and fast identification of non-covalent interactions between biological macromolecules and their ligands. available at <https://plip-tool.biotec.tu-dresden.de/plip-web/plip/index>.
 31. Geary, W.J. The use of conductivity measurements in organic solvents for the characterization of coordination compounds. *Coord. Chem. Rev.* **1971**, 7, 81-122
 32. Kohútová, M. Magneto-chemical investigation of trichloro (aliphatic alcohol) titanium (III) complexes. *Chem. Pap.* **1979**, 33, 187-196.
 33. Kumar, M.; Saxena, P. Transition metal complexes of 5-bromo salicylaldehyde-2-furoic acid hydrazide: Synthesis and characterization. *Orient. J. Chem.* **2012**, 28, 1927-1931.
 34. Mahto, C.B. Study of complex compounds of transition metals with isonicotinic acid hydrazides. *J. Indian Chem. Soc.* **1980**, 57, 485-489.
 35. Rastogi, R.K.; Sharma, S.; Rastogi, G.; Singh, A.K. Synthesis and characterization of Ti(III), V(III), VO(IV), MoO(V), Fe(II) and Fe(III) complexes of benzil-2,4-dinitrophenyl hydrazone *p*-bromo aniline. *Green Chem. Tech. Lett.* **2016**, 2, 177-179.
 36. Ghani, U.; Ullah, N. New potent inhibitors of tyrosinase: Novel clues to binding of 1,3,4-thiadiazole-2(3*H*)-thiones, 1,3,4-oxadiazole-2(3*H*)-thiones, 4-amino-1,2,4-triazole- 5(4*H*)-thiones, and substituted hydrazides to the dicopper active site. *Bioorg. Med. Chem.* **2010**, 18, 4042-4048.
 37. Gasowska, B.; Frackowiak, B.; Wojtasek, H. Indirect oxidation of amino acid phenyl hydrazides by mushroom tyrosinase. *Biochim. Biophys. Acta-General Subjects* **2006**, 1760, 1373-1379.
 38. Muller, G.H.; Waldmann, H. The phenyl hydrazide as an enzyme-labile protecting group-oxidative cleavage with mushroom tyrosinase. *Tetrahedron Lett.* **1999**, 40, 3549-3552.
 39. Gastel, M.V.; Bubacco, L.; Groenen, E.J.J.; Vijgenboom, E.; Canters, G.W. EPR study of the dinuclear active copper site of tyrosinase from *Streptomyces* antibiotics. *FEBS Lett.* **2000**, 474, 228-232.
 40. Jiménez, M.; García-Carmona, F. The effect of sodium dodecyl sulphate on polyphenol oxidase. *Phytochemistry* **1996**, 42, 1503-1509.
 41. Moore, B.M.; Flurkey, W.H. Sodium dodecyl sulfate activation of a plant polyphenol oxidase. Effect of sodium dodecyl sulfate on enzymatic and physical characteristics of purified broad bean polyphenol oxidase. *J. Biol. Chem.* **1990**, 265, 4982-4988.
 42. Escribano, J.; Cabanes, F.; Garcia-Carmona, F. Characterization of latent polyphenol oxidase in table beet: Effect of sodium dodecyl sulphate. *J. Sci. Food. Agric.* **1997**, 73, 34-38.

43. Smart, B.E.; Hudlicky, M.; Pavlath, A.E. Chemistry of organic fluorine compounds II. *Crit. Rev.* 1995, 187, 979.
44. Pillaiyar, T.; Manickam, M.; Namasivayam, V. Skin whitening agents: medicinal chemistry perspective of tyrosinase inhibitors. *J. Enz. Inhib. Med. Chem.* **2017**, 32, 403-425.
45. Radhakrishnan, S.K.; Shimmon, R.G.; Conn, C.; Baker, A.T. Azachalcones: A new class of potent polyphenol oxidase inhibitors. *Bioorg. Med. Chem. Lett.* **2015**, 25, 1753-1756.
46. Yi, W.; Cao, R.; Peng, W.; Wen, H.; Yan, Q.; Zhou, B.; Ma, L.; Song, H. Synthesis and biological evaluation of novel 4-hydroxybenzaldehyde derivatives as tyrosinase inhibitors. *Eur. J. Med. Chem.* **2010**, 45, 639-646.
47. Gencer, N.; Sonmez, F.; Demir, D.; Arslan, O.; Kucukislamoglu, M. Synthesis, structure-activity relationships and biological activity of new isatin derivatives as tyrosinase inhibitors. *Curr. Top. Med. Chem.* **2014**, 14, 1450-1462.
48. Kemal, C.; Louis-Flamberg, P.; Krupinski-Olsen, R.; Shorter, A.L. Reductive inactivation of soybean lipoxygenase 1 by catechols: a possible mechanism for regulation of lipoxygenase activity. *Biochemistry*, **1987**, 26, 7064-7072.
49. Van der Zee, J.; Eling, T.E.; Mason, R.P. Formation of free-radical metabolites in the reaction between soybean lipoxygenase and its inhibitors. An ESR study. *Biochemistry*, **1989**, 28, 8363-8367.
50. Kovala-Demertzi, D.; Hadjipavlou-Litina, D.; Staninska, M.; Primikiri, A.; Kotoglou, C.; Demertzi, M.A. Antioxidant, *in vitro*, *in vivo* antiinflammatory activity and antiproliferative activity of mefenamic acid and its metal complexes with manganese(II), cobalt(II), nickel(II), copper(II) and zinc(II). *J. Enzyme Inhib. Med. Chem.* **2009**, 24, 742-752.